Research Article

Tidal Energy-based Optimal Microgrid Planning with the Presence of Electric Vehicles

Farshad Heidarpour [a]* , Rostam Izadpour [b],
Vahid Imani [c]

[a] PhD student in Power Electrical Engineering, Isfahan Free University (Khorasgan) Chahar Mahal and Bakhtiari Power Distribution Company, Iran. Farshadh39@Gmail.com
[b] Deputy of Operation and Dispatching of Electricity Distribution Company, Master of Electrical Power Engineering, Chahar Mahal and Bakhtiari Power Distribution Company, Iran. Rizadpour@Gmail.com
[c] Director of the Office of the Board of Electricity Distribution Company, Master of Electrical Power Engineering, Chahar Mahal and Bakhtiari Power Distribution Company, Iran vahidimaniii55@gmail.com

Article History: Received: 5 April 2021; Accepted: 14 May 2021; Published online: 22 June 2021

Abstract: The development of clean and renewable energy has led to modern planning and operation of power systems. Tidal energy is seen as one of the newest energy resources used to generate electrical power. In power generation systems, the tides in a river direct seawater flow towards hydraulic turbines and generate electric power through conventional induction or doubly-fed induction generators (DFIG). These electric power generation systems can be utilized in the form of coastal microgrids including electric charges, storage systems, and plug-in electric vehicles (PEVs). Although the velocity and direction of water flow in tidal energy systems are predictable, its variability hinders its utilization in the form of coastal microgrids. On the other hand, since electric vehicle parking lots can serve as part of the charging or generation system in the coastal microgrids, and also considering the fact that the random behavior of drivers makes power consumption or generation of parking lots random in nature, it will be highly important to optimally design these parking lots and storage systems.

This research sought to optimize the performance of a coastal parking lot integrated with tidal energy generation systems, which serve as an independent microgrid. An optimization problem is aimed at maximizing microgrid revenue and minimizing tidal energy loss along with practical microgrid constraints including island performance stability and equipment utilization constraints.

Keywords: tidal power plant, microgrid, planning, energy storage system

1. Introduction

The growing global population and social and economic development have led to increased demands for energy across the world. A major part of this demand is met by fossil fuels, which lead to greenhouse gas emissions and climate and environmental changes. Therefore, it is necessary to increase the share of renewable energy resources to meet global energy needs. Included in renewable energies is tidal energy which is a regular, predictable, and stable source of energy. Globally, tidal energy sources which are technically used and are close to coastlines are estimated by several sources to be around 1 terawatt. In some areas, the potential for tidal current technologies is sometimes greater than that when it comes to dam construction methods. Having extended coastlines, a growing population, rising energy needs, and extreme air pollution, Iran has the potential to expand into marine energy sources. Fortunately, efforts are being made in this connection in Iran, a country that enjoys several thousand kilometers of marine borders and coastlines. The current Iranian energy model is based on fossil fuels, and transformation into a different and stable model requires an expansion of renewable energy resources. In this section, a thorough study has been carried out to examine the tidal energy potential in Iran, which can be used to identify the optimal locations for the utilization of marine energy. The Caspian Sea is considered to be the largest sea in the world which has a low tide and can only absorb energy from the waves as it does not meet the minimum tidal energy conditions (Khojasteh, Kamali & Bineh, 2017, 8). The tidal amplitude in this sea is less than five meters while the tidal flow velocity is less than two meters per second. Accordingly, this study addresses the southern coasts, the Persian Gulf, and the Gulf of Oman. Research has also demonstrated the southern seas of Iran as the best locations for receiving tidal energy. Therefore, one would say that there are different energy locations with high potential for marine energy development in the Persian Gulf and the Gulf of Oman, though, this potential has received little attention.

Also, the use of energy in today's modern world is a significant issue that affects human life. The energy which is stored and reused assumes significance. Renewable energies can greatly contribute to the future of humanity and its survival [1]. Tidal turbines have, in recent years, played a critical role in the development of technology, ushering in many possibilities for human beings [2].

These power plants have some advantages in the way that they have predictable reversible sources and could have a longer lifespan if properly designed and constructed. In other words, tidal power is a renewable energy resource, and such power plants, unlike fossil fuels, do not cause any pollution or greenhouse gases. Moreover, they do not need much repair or fuel.

The exploitation of this energy does not depend on climatic conditions. Water transfers a great deal of energy as it has high density, and for this, it is more useful than wind energy, thus yields higher efficiency. When dams are

constructed to utilize tidal energy, they do protect the long coastlines from high tides and extreme turbulent storms. Tidal turbines have played a critical role in expanding technology in recent years. Tidal currents help tidal turbines to generate electricity because they can receive large amounts of energy [3]. Over the past 20 years, researchers have been performing research on horizontal axis tidal current turbines, but scant research was focused on the efficiency of wave and current turbines performance. Barlathrope [4] examined the effect of waves on the properties of tidal current turbines. A horizontal axis turbine with blades was tested in a tug tank and the mean torque range at a regular wave was measured. The findings, within a wave period, demonstrated that all the mean values of the measured parameters were found to be the same as the waveless conditions, though the torque variations were evident.

Speaking of grid systems, electric vehicles can be a consumer or a generator of power [2]. PEVs charging optimization has been studied in many types of research. To model reduced operational costs, the general computational method is to create an optimization problem, such as nonlinear programming and mixed integrated programming (MIP). Structured problems can be solved using evolutionary algorithms (particle swarm optimization), control strategy (fuzzy control), and so on.

Fernandez [5] proposed an intermediate operational model that included two phases. In the first phase, the operating costs would be reduced by using a temporal scale of one day a year. In the second phase, the previously adjusted schedule (through solving the optimization problem) was modified according to the unit outages, also derived from the Monte Carlo method.

Lee et al. [6] used a hierarchical control algorithm to reduce power generation costs from EVs charging demand to coordinate oscillating power generation via wind energy. This hierarchical control algorithm was divided into three levels of different temporal scales. The first-level controller solves the wind energy schedule and conventional energy utilization on a one-hour scale. EVs intermediate controller schedule secures hourly demands. The bottom-level controller uses the power grid frequency deviation to generate EVs real-time control. Conventional energy planning and wind energy consumption should first be modeled as a knapsack problem. This allows researchers to use dynamic programming as a solution.

Vaya and Anderson [7] sought to reduce generation costs from a different perspective. In their research, EVs batteries were used as distributed storage to coordinate RESs oscillation. EVs instability was modeled as potential storage in which the SOC depended on discrete patterns. They formulated the problem as the Optimal Power Flow (OPF) problem, which integrated the possible model of wind energy generation. Oscillations from wind energy generation can be offset by changing the EVs charging systems. The researchers then used a Swiss transmission system for simulation. For OPF, they consolidated the data collected from major power channels, extended wind power generation data, and made predictions according to the National Renewable Energy Laboratory.

Vasirani et al. [8] proposed an effective plan for power suppliers to increase profits. To meet this goal, the researchers examined the feasibility of using EVs as a storage means. In this connection, they used the virtual power plant (VPP) of the wind station to create a separate entity composed of multiple power suppliers and EVs in the electricity market. The profits from VPP were modeled through linear programming. This problem was solved through the old simplification technique. In the case study, researchers used data from real wind energy generation and electricity prices to collect data on wind speed and turbine parameters in Spain.

In [9] the problem was monitored from the price-supply-demand perspective. When RESs had greater influence, RESs oscillations could affect the price of electricity in a variety of ways. The researchers used several approaches to balance the demand for EVs, increase the contribution of RESs, and consider the distribution capacity of the grid. They then concentrated on density issues in the distributed energy system to identify the optimal charging strategy. Moreover, three density mechanisms were introduced, which included dynamic grid tariffs, assigned advanced capacity, and the distribution grid market.

In power generation systems, the tides in a river direct seawater flow towards hydraulic turbines and generate electric power through conventional induction or doubly-fed induction generators (DFIG). These electric power generation systems can be utilized in the form of coastal microgrids including electric charges, storage systems, and plug-in electric vehicles (PEVs). Although the velocity and direction of water flow in tidal energy systems are predictable, its variability causes barriers to its utilization in the form of coastal microgrids. On the other hand, since electric car parking lots can serve as part of the charging or generation system in the coastal microgrids, and also considering the fact that the random behavior of drivers makes power consumption or generation of parking lots random in nature, it will be highly important to optimally design these parking lots and storage systems.

This research sought to optimize the performance of a coastal parking lot integrated with tidal energy generation systems, which serve as an independent microgrid. An optimization problem is aimed at maximizing microgrid

revenue and minimizing tidal energy loss along with practical microgrid constraints including island performance stability and equipment utilization constraints.

2. Research Methods

EV models

Electric vehicles can operate in grid-to-vehicle (G2V) and vehicle-to-grid (V2G) modes. In this study, EV owners were encouraged to participate in the V2G program through incentives provided by the IPL director. The vehicles taking part in the V2G program are called V2G vehicles and other G2V vehicles.

When an electric vehicle is plugged into the grid, the charging status depends on the charging status in the previous time interval while the charging or discharging rate in that interval is as follows [10]:

$$\boldsymbol{SOC_v^t = SOC_v^{t-\Delta t} + \left(\frac{\eta_c^v P_{v.c}^t}{C^v} - \frac{P_{v.d}^t}{\eta_d^v C^v}\right) \times \Delta t;\ t_v^a < t \le t_v^d}$$

(1)

Where $P_{v.c}^t$ and $P_{v.d}^t$ represent the battery charging and discharging capacity. η_c^v and η_d^v also represent the charge/discharge efficiency of the battery. Moreover, C^v indicates the battery capacity, t_v^a and t_v^d the time at which electric vehicles arrive at or depart from the parking lot.

IPL revenues and costs when exchanging energy for PEVs

The IPL understudy yields the following revenues and incurs costs when energy is exchanged for PEVs:

* Revenue from selling energy to G2V vehicles

* Revenue from selling energy to V2G vehicles

* Costs of buying energy from V2G vehicles

* Costs of using the available capacity of V2G vehicles

* Cost of penalty from V2G vehicle charging needs unmet.

Revenue from selling energy to G2V vehicles is calculated as follows [11]:

$$\boldsymbol{R_{PEV-m_{G2V}}^t = \sum_{v=1}^{m_{G2V}} (P_{v.c}^t \times \rho_c^t) \times \Lambda_v^t \times \Delta t}$$

(2)

Where $P_{v.c}^t$ represents the vehicle charging power, ρ_c^t is the energy price in a relevant period and Λ_v^t is the binary variable indicating the presence or non-presence of the vehicle in the lot. m_{G2V} also represents total G2V vehicles.

Concerning V2G vehicles, the charge status by the time the vehicle leaves the parking lot ($SOC_{t_v^d}$) determines whether the vehicle is a seller or buyer of energy. If the final SOC is less than the initial SOC, the vehicle turns out to be a seller of energy, otherwise, the vehicle is a buyer.

Revenue from selling energy to V2G vehicles is calculated as follows [11]:

$$\boldsymbol{R_{PEV-m_{V2G}}^t = \sum_{v=1}^{m_{V2G}} \left(SOC_{t_v^d} - SOC_{t_v^a}\right) \times C^v \times \rho_{c.V2G}^t \times \tau_v^d}$$

(3)

Where $SOC_{t_v^d}$ and $SOC_{t_v^a}$ represent the final and initial SOCs, respectively. $\rho_{c.V2G}^t$ represents the energy price for V2G vehicles in a relevant period, m_{V2G} suggests the total V2G vehicles and τ_v^d represents a marker (flag) variable indicating the vehicle leaving the lot.

If the final SOC is less than the initial SOC, the costs of buying energy from V2G vehicles is as follows:

(4)

$$C^t_{PEV-m_{V2G}} = \sum_{v=1}^{m_{V2G}} \left(SOC_{t^a_v} - SOC_{t^d_v}\right) \times C^v \times \rho^t_{d.V2G} \times \tau^d_v$$

Where $\rho^t_{d.V2G}$ is the discharge price of V2G vehicles.

Moreover, the smart parking lot will undertake the costs from using the free capacity of electric vehicle batteries as follows:

(5) $$C^t_{Cap-V2G} = \sum_{v=1}^{m_{V2G}} (SOC^{max}_v - SOC^{min}_v) \times C^v \times \rho^t_{cap.V2G} \times \Lambda^t_v$$

Where SOC^{max}_v and SOC^{min}_v are the maximum and minimum SOC values of each vehicle and $\rho^t_{cap.V2G}$ represents the price of using the free power of V2G vehicle batteries in a relevant period.

If the final charge of the vehicle turns out to be less than the minimum amount required and its delivery is low, the smart parking lot must pay for the owner for the unmet need to charging V2G vehicles as follows:

(6)

$$C^t_{Penalty} = \sum_{v=1}^{m_{V2G}} \left(SOC^{desired}_v - SOC^{t_d}_v\right) \times C^v \times \rho_{Penalty} \times \tau^d_v$$

Where $SOC^{desired}_v$ represents the desired charge level and $SOC^{t_d}_v$ is the penalty for unmet desired charge level.

Objective function

Decision variables

Decision variables include the following:

- Upstream grid-modeled power
- Charging or discharging power of V2G vehicles
- Charging power of G2V vehicles
- Hydrogen unit-exchanged power

The variables that entered the optimization problem during one day (24 hours) are as follows:

(7)

$$H = \begin{bmatrix} P^1_{v1} & P^1_{v2} & \dots & P^1_{mg2v} & \dots & P^1_{mv2g} & P^1_H \\ P^2_{v1} & P^2_{v2} & \dots & P^2_{mg2v} & \dots & P^2_{mv2g} & P^2_H \\ \vdots & & & & & & \vdots \\ P^{24}_{v1} & P^{24}_{v2} & \dots & P^{24}_{mg2v} & & P^{24}_{mv2g} & P^{24}_H \end{bmatrix}$$

Profit function

The profit function of the smart parking includes a sum of the difference between parking revenues and costs in all periods and is calculated as follows:

(8)

$$Profit = \sum_{v=1}^{T=24} \Big[\left(\left(P^t_{sell-grid} \times \rho^t_{grid}\right) - \left(P^t_{buy-grid} \times \rho^t_{grid}\right)\right) \times \Delta t + \left(\rho^t_{sell-load} \times P^t_L\right) \times \Delta t + \left(R^t_{PEV-m_{G2V}} + R^t_{PEV-m_{V2G}}\right) - \left(C^t_{PEV-m_{V2G}} + C^t_{Cap-V2G} + C^t_{Penalty}\right) - \left(C_{FC}(t) + C_{EL}(t) + C_{Tank}(t)\right)\Big]$$

Where $P^t_{sell-grid}$ and $P^t_{buy-grid}$ represent the power sold and bought from the upstream grid. P^t_L represents the amount of charging power in each time interval and $\rho^t_{sell-load}$ indicates the price of selling energy for an electrical charge in each time interval. In the above relation, C_{FC}, C_{EL} and C_{Tank} indicate the costs of utilization, repair, and maintenance of the fuel cell, electrolyzer, and hydrogen tank, respectively.

This research used the Monte Carlo algorithm to model the uncertainty about charging, tidal power generation, and behavior of vehicle driver with its average output used in the calculations [12].

The objective function is so designed to observe the maximized profit function and the system constraints:

(9)

$$\boldsymbol{OF} = \max_{\boldsymbol{H}} \ (\boldsymbol{Profit})$$

Constraints

The IPL is assumed to be connected to the upstream grid using a connection line and the following conditions must be followed [7, 12-15]:

(10)

$$\boldsymbol{P^t_{IPL-EL} + P^t_L + P^t_c + P^t_{sell-grid} = P^t_{FC-IPL} + P^t_{buy-grid} + P^t_d}$$

(11)

$$\boldsymbol{\left|P^t_{grid}\right| \leq P_{grid-max}}$$

(12)

$$\boldsymbol{SOC^{max}_v \leq SOC^t_v \leq SOC^{min}_v}$$

(13)

$$\boldsymbol{-P^{max}_{v,d} \leq P^t_v \leq P^{max}_{v,c}}$$

(14)

$$\boldsymbol{-P^{max}_{EL} \leq P^t_H \leq P^{max}_{FC}}$$

(15)

$$\boldsymbol{M^t_{Tank} \leq M_{max}}$$

Where P^t_c and P^t_d indicate the total charge and discharge power of electric vehicles.

In the above relations $\boldsymbol{P_{grid-max}}$ represents the maximum power to pass through the connection line. $\boldsymbol{P^{max}_{v,c}}$ and $\boldsymbol{P^{max}_{v,d}}$ indicate the maximum charge and discharge power of the battery. Also, $\boldsymbol{P^{max}_{EL}}$ and $\boldsymbol{P^{max}_{FC}}$ represent the maximum power of the electrolyzer and the fuel cell. Finally, $\boldsymbol{M_{max}}$ is the maximum storage capacity in a hydrogen tank.

To remove the effect of the initial storage of the hydrogen tank from the calculations, the amount of hydrogen storage in the first and last hour of the day is regarded as the same:

(16)

$$\boldsymbol{M^0_{Tank} = M^{24}_{Tank}}$$

The cost of utilization, maintenance, and repair of IPL equipment is modeled by the following relation [13]:

(17)

$$\boldsymbol{C^t = \left(\frac{\left(\frac{\gamma(1+\gamma)^n}{(1+\gamma)^n - 1} \right) \times A}{CF \times 8760 \times P_{rated}} \times P^t + C_M \right)}$$

Where $\boldsymbol{C_M}$ represents the cost of maintenance and repairs in terms of ($/year), $\boldsymbol{CF}$ the capacity coefficient, $\boldsymbol{A}$ the cost from the initial investment ($), $\boldsymbol{n}$ the lifespan, and $\boldsymbol{\gamma}$ the interest rate. Also, $\boldsymbol{P_{rated}}$ and $\boldsymbol{P^t}$ are the rated power and field power of equipment in IPL, respectively.

PSO algorithm working mechanism

Particle swarm optimization begins with a category of random answers (particles) and then updates the generations to search in order to find the optimal solution in a problem space. Each particle is multidimensionally represented by two values of $\mathbf{V_{id}}$ and $\mathbf{X_{id}}$ (the former is the velocity and the latter the position of the i^{th} particle in the d^{th} dimension). At each stage of the mass movement, each particle is updated according to two best personal and global values.

The first value, the best personal value, represents the best answer in terms of fitness currently obtained for each particle. This value is known as **PBest**. Also, the best global value of particles is called **GBest**, being one of the main parameters of particle swarm optimization. It should be noted, however, that both mentioned values should be stored.

If a particle participates as a population in a local neighborhood, the **GBest** value is calculated in the same neighborhood, which is so-called the best location represented by **LBest**.

One of the key and appealing aspects of the particle swarm optimization technique is its simplicity, which includes only two models of velocity and location equations, where the coordinates of each particle show a possible solution related to two vectors [14].

The velocity and location equations can be calculated by means of **PBest** and **GBest** values, as follows:

(17)

$$\boldsymbol{V_i^{k+1} = \omega\, v_i^k + c_1 r_1 \left(PBest_i{}^k - x_i^k\right) + c_2 r_2 \left(GBest^k - x_i^k\right)}$$

(3-24)

$$\boldsymbol{X_i^{k+1} = x_i^k + v_i^{k+1}}$$

Where $\mathbf{c_1}$ and $\mathbf{c_2}$ are two positive constant values. $\mathbf{r_1}$ and $\mathbf{r_2}$ are two random values of uniform distribution in the [1-0] range. ω is also the inertia weight selected as follows:

(18)

$$\boldsymbol{\omega = \omega_{max} - \frac{\omega_{max} - \omega_{min}}{iter_{max}} \times iter}$$

Also, other references have considered various formulas for **ω** such as the following formula [69]:

(19)

$$\boldsymbol{\omega = (\omega_{initial} - 0.5) \times (iter_{max} - iter) + 0.5}$$

Where $\boldsymbol{\omega_{initial}}$ is 0.95. The reason why there are different formulas is that convergence in particle swarm optimization is highly dependent on the **ω** value, and depending on the system and type of particle swarm optimization, a unique **ω** value is used. An appropriate **ω** value causes a balance between local and global searches. Practical results suggest that it is better to consider a greater value of **ω** in the initial stages, to perform a thorough and global search of the search space. Then, when the algorithm is run, the **ω** value is gradually reduced to get the algorithm closer to the convergence limit and to obtain more accurate answers. Considering **ω** as the fluid coefficient of the environment, a greater **ω** value means that the movement in the environment takes place smoothly, with the particles facing more viscosity. In this case, it becomes possible for particles to greatly converge to the optimal points. For instance, considering a value of 0.9 for **ω** and its gradual reduction to zero can be a good way to solve most problems.

PSO algorithm Flowchart

IPL was optimized by particle swarm algorithm in MATLAB software. The optimization flowchart is illustrated in Figure (1-4). Initially, charge demand, tidal power plant generation, and the driving and parking pattern of electric

vehicles enter as input. The objective function is then optimized using the PSO algorithm [15]. Thus, the optimal utilization pattern of smart parking is obtained.

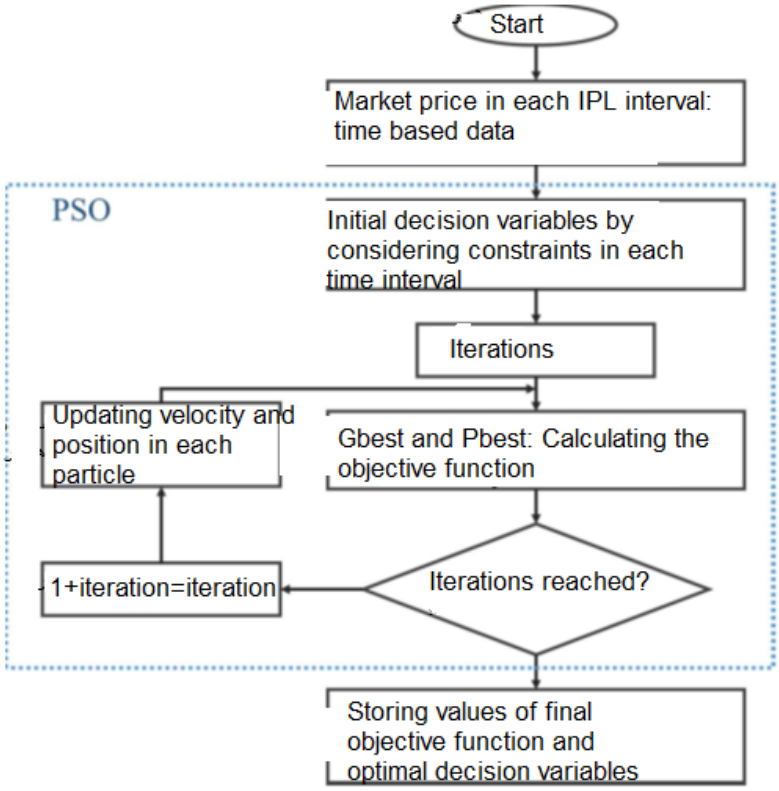

Figure 1: Flowchart of optimization

Input data

The profile predicted based on the market price is illustrated in Figure 2a. The specific electric charge demand is also shown in Figure 2b. Figure 2 demonstrates the projected output of the tidal power plant during the 24 hours under study.

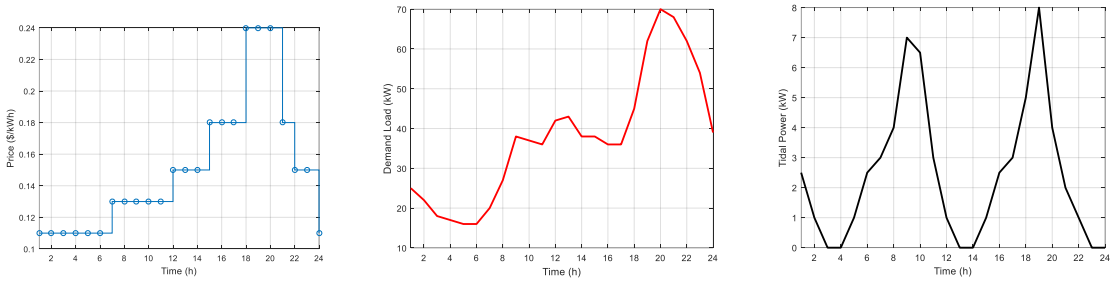

a b c

Figure 2: a) Profile predicted based on the market price [12], b) Load demand during 24 hours, c) Projected power plant tidal power generation profile [12]

The price of energy sold to electric charge is 30% higher than the market price with the interest rate standing at 5%. The technical features of the hydrogen unit and the IPL economic considerations are provided in Table 1.

Ten electric vehicles took part in the V2G program while 5 electric vehicles went to the parking lot during the day for desired charging (G2V). All vehicles under study are considered to have the same technical features. These technical specifications are summarized in Table (1). The maximum electric power converter power, which is responsible for charging and discharging the vehicle battery, is taken to be 4 kWs. Table (1) shows the charging tariffs of G2V vehicles as well as the charging and discharge tariffs, tariff on free battery capacity use, and penalty tariff for failure to meet the desired charge level in V2G vehicles. The optimum SOC of V2G vehicles is obtained

when vehicles leave the parking lot. Some predicted values are considered for arriving at the parking time, leaving the parking lot while the initial charge level of G2V vehicles are given. These values are provided for V2G vehicles.

Vehicle input data

Table 1: Technical specifications of the vehicles understudy

PHEV	Battery Lithium-Ion *kWh*	η_c^v %	η_d^v %	SOC_{min} %	SOC_{max} %
NISSAN LEAF®	24	90	95	15	95

Table 2: Electric vehicle charging tariff

ρ_c^t	$\rho_{c,V2G}^t$	$\rho_{d,V2G}^t$	$\rho_{cap,V2G}^t$	$\rho_{Penalty}$
\$/kWh $1.3\times \rho_{grid}^t$	\$/kWh $1.1\times \rho_v^{plug\_in}$	\$/kWh $1\times \rho_v^{plug\_in}$	\$/kWh $0.02\times \rho_{grid}^t$	\$/kWh $4\times \rho_v^{plug\_in}$

Table 3: Desired SOC of V2G vehicles when leaving the parking lot

PHEV (v)	1	2	3	4	5	6	7	8	9	10
$SOC_v^{desired}$ (%)	90	60	90	85	75	75	55	70	90	60

Table 4: Projected G2V vehicles values

PHEV (v)	t_a^v	t_d^v	SOC_{ta}^v
1	7:13	13:11	45.59
2	9:10	15:20	22.04
3	9:35	15:50	27.3
4	7:35	18:50	40.36
5	12:07	21:45	16.47

Table 5: Projected G2V vehicles values

PHEV (v)	t_a^v	t_d^v	SOC_{ta}^v
1	7:10	15:33	50
2	8:55	17:55	31.6
3	6:20	15:25	42.9
4	8:12	16:43	48.2
5	8:05	13:46	42.5
6	7:46	17:05	37.8
7	9:55	13:40	48.5
8	5	16:30	33
9	6:10	14:40	63
10	7:42	13:50	46.3

3. Simulation results

Scenario 1 - Base system (without power plant)

In this case, the base system is considered without a tidal power generation plant.

The charging and discharging of electric vehicles are illustrated in Figure (2b). According to output data, the IPL charging was 42 kW at 12 o'clock, and the power bought from the upstream grid was 54.44 kW. The fuel cell generation power at this hour was 0 kW and the net power received from electric vehicles stood at -12.11 kW. At this hour, the charging power of V2G cars was 20 kW with their discharging power being 19.88 kW; in the meantime, the charging power of G2V vehicles stood at 12 kW at this hour.

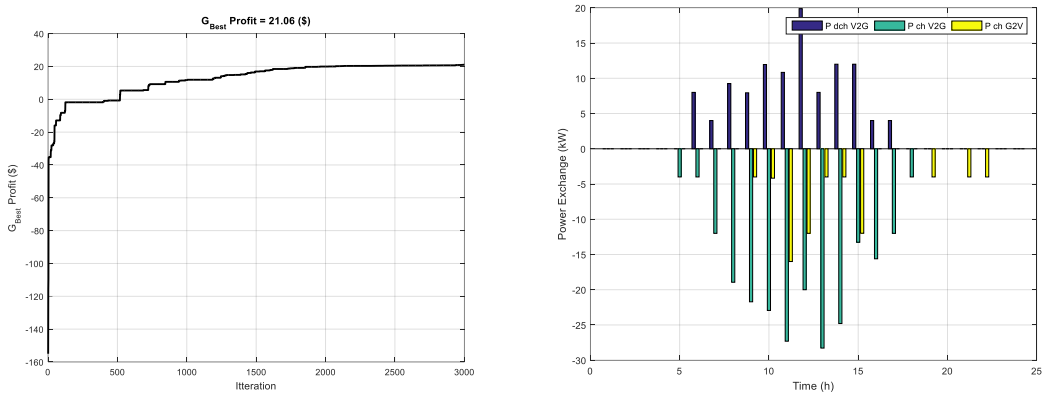

a b

Figure 2- a) Optimization process by PSO algorithm, b) Charging and discharging of electric vehicles

Scenario 2 - System with a power plant

In this case, the system involves a tidal power generation plant. Figure 3a demonstrates the optimization process by the PSO algorithm. Looking at this figure, it is seen that the IPL's daily profit has risen to 35.03$, up 66% from the first scenario, indicating we achieved a good and optimal answer. We saw in the PSO algorithm that the optimization answers also tend to positive from negative.

Charging and discharging of electric vehicles, taking into account the presence of a tidal power plant, is seen in Figure 3b. It is clear that the parking lot has been used from 7 am to 10 pm, during which the exchanges of vehicles with IPL have taken place.

In this state, because of tides from 3 pm to 10 pm, the charging power of G2V vehicles has been transferred to this timing. V2G vehicles discharging took place from 6 am to 5 pm while V2G vehicles charging at 5 am to 5 pm; is while G2V vehicles charging took place at 8 am to 10 pm.

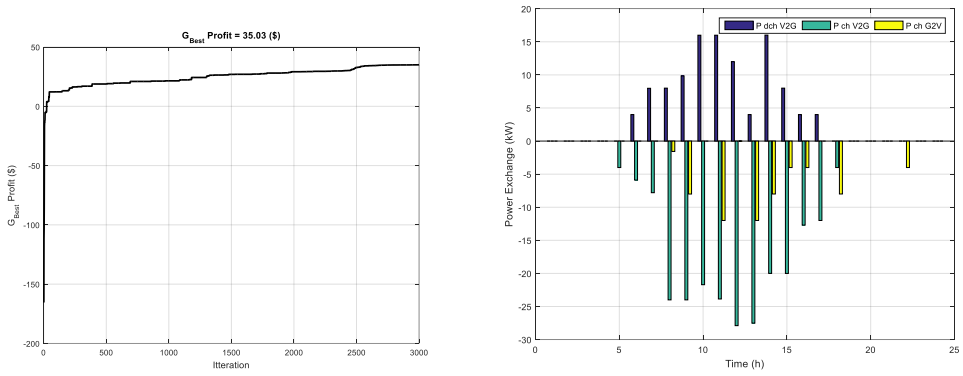

a b

Figure 3- a) Optimization process by PSO algorithm involving a tidal power plant, b) Charging and discharging of electric vehicles involving a tidal power plant

Comparison of simulation scenarios

Figure 4 illustrates a comparison of two simulation scenarios based on the optimization process by the PSO algorithm. As stated earlier, the second scenario yielded a 66% rise in revenue, indicating that we tended to a positive and acceptable answer in terms of optimization, considering that our daily profit rose to 66% compared to the first scenario.

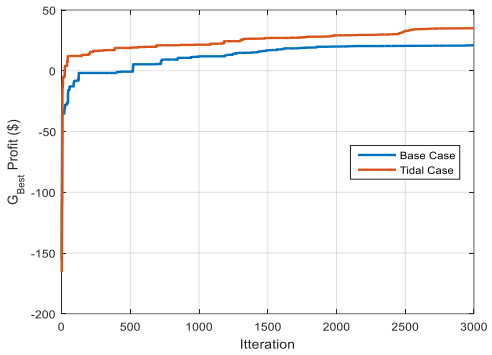

Figure 4: Comparison of two simulation scenarios from the perspective of optimization process by PSO algorithm

Figure 5 demonstrates the comparison of two simulation scenarios based on the optimal programming findings. In the first figure, the power exchanged with the upstream grid is compared in the two scenarios. The second and third figures illustrate the fuel cell power and the electrolyzer power in the first and second scenarios, respectively. Figure 4 conducts a comparison of the power delivered to electric vehicles in the two scenarios. In the first figure, according to the two scenarios, the grid power, and in the second figure, the power the fuel cell delivers to the IPL are shown. Also, changes are evident in the third figure demonstrating the power that IPL delivers to the electrolyzer.

Figure 6 compares the two simulation scenarios in terms of the charging and discharging of electric vehicles. As seen in this figure, when tidal power plant generation is higher, the charging power consumed by vehicles also increases.

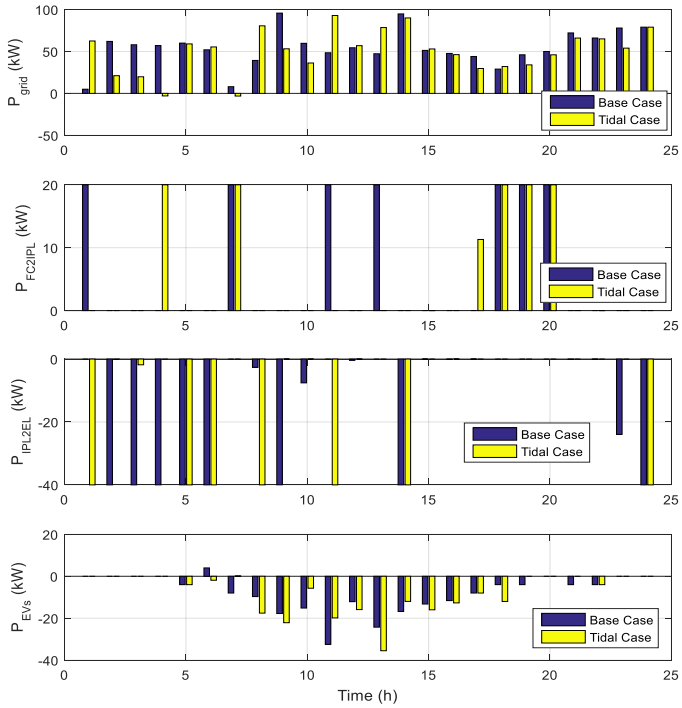

Figure 5 - Comparison of two simulation scenarios from the perspective of optimal planning results

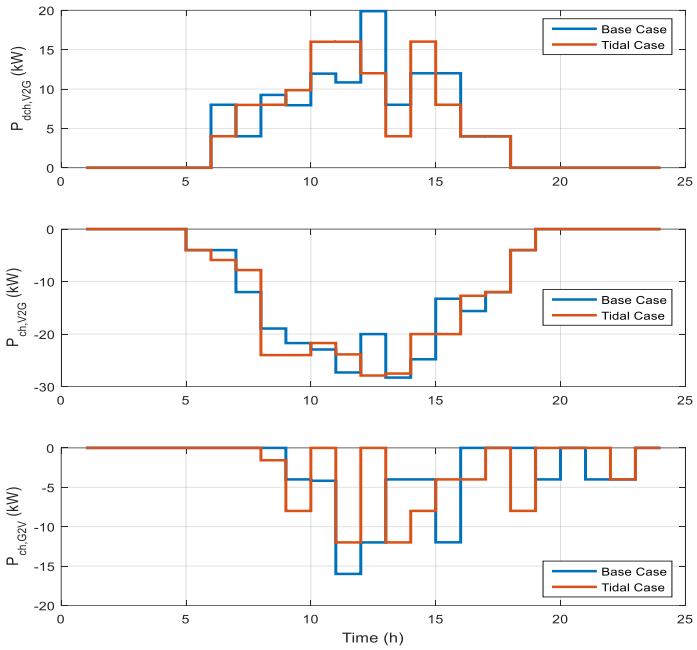

Figure 6 - Comparison of two simulation scenarios from the perspective of charging and discharging results of electric vehicles

Finally, Figure 7 illustrates a comparison of the two simulation scenarios based on the hydrogen tank storage results over 24 hours. The hydrogen storage level in the last hours of the day rose due to a rise in a free tidal generation. This prevents the purchase of energy from the upstream grid and helps the overall revenue of the IPL system. In the two-scenario system, when the fuel cell was operating, hydrogen reduction in the storage tank changed and when the electrolyzer was operating, the hydrogen tank level changed due to the increase in the two-scenario scenario results.

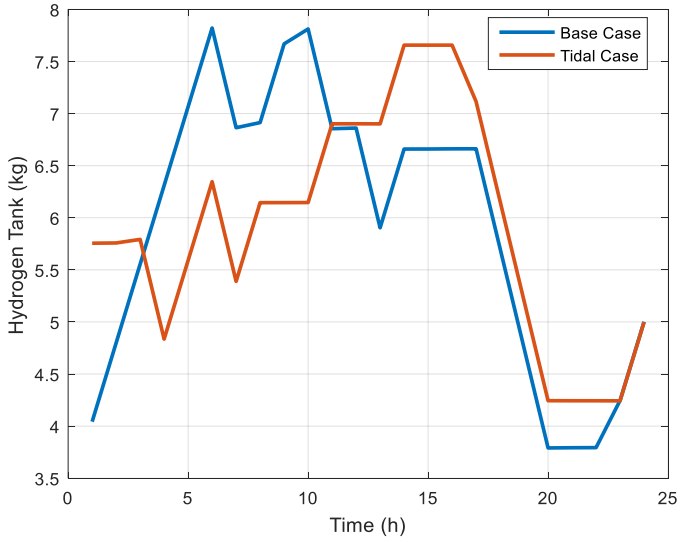

Figure 7 - Comparison of two simulation scenarios based on hydrogen tank storage results during 24 hours

4. Conclusion

This study introduced a new model for charging and discharging electric vehicles in a coastal microgrid involving a tidal power plant and an energy storage system. A proposed formulation was used for a smart coastal parking lot. Numerical findings suggested the efficiency of the method in this dissertation.

Also, a new approach for charging and discharging electric vehicles was applied in this dissertation to take into account the uncertainties in charging demand, driver behavior, energy prices, and tidal power plant generation resulting from a final optimization. Numerical results indicated that the proposed method was economically optimal, complying with the technical constraints of the system.

Given the capability of the southern ports in the country, we selected one of the ports as an instance. We determined the base (minP.Q) and (maxP.Q) levels to perform analytical modeling.

By distributing load and consumption, the required minimum and maximum limits were obtained.

For these limits, a necessary economic analysis was carried out (for profit and loss analyses).

The necessary functions for this were determined:

- Upstream-grid modeled power
- Charging and discharging power
- Hydrogen unit-exchanged power
- Profit functions
- Constraints

Using the particle swarm algorithm, and providing a suitable probability function, the convergence form of the algorithm was solved.

In the simulation of the results, the optimization performed was shown in relation to the previous system.

In the first case, the charging and discharging approaches were not used, as was demonstrated by introducing a probability function.

References

1. J. Massiani, "Cost-Benefit analysis of policies for the development of electric vehicles in Germany: Methods and results," Transport Policy, vol. 38, pp. 19-26, 2015.
2. S. Shahidinejad, S. Filizadeh, and E. Bibeau, "Profile of charging load on the grid due to plug-in vehicles," Smart Grid, IEEE Transactions on, vol. 3, no. 1, pp. 135-141, 2012.
3. S. Soylu, Electric Vehicles: The Benefits and Barriers. InTech, 2011.
4. W. Kempton, J. Tomic, S. Letendre, A. Brooks, and T. Lipman, "Vehicle-to-grid power: battery, hybrid, and fuel cell vehicles as resources for distributed electric power in California," Institute of Transportation Studies, 2001.
5. C. Fernandes, P. Frías, and J. M. Latorre, "Impact of vehicle-to-grid on power system operation costs: the Spanish case study," Applied energy, vol. 96, pp. 194-202, 2012.
6. C.-T. Li, C. Ahn, H. Peng, and J. Sun, "Integration of plug-in electric vehicle charging and wind energy scheduling on electricity grid," in 2012 IEEE PES Innovative Smart Grid Technologies (ISGT), 2012, pp. 1-7: IEEE.
7. M. G. Vayá and G. Andersson, "Integrating renewable energy forecast uncertainty in smart-charging approaches for plug-in electric vehicles," in PowerTech (POWERTECH), 2013 IEEE Grenoble, 2013, pp. 1-6: IEEE.
8. M. Vasirani, R. Kota, R. L. Cavalcante, S. Ossowski, and N. R. Jennings, "An agent-based approach to virtual power plants of wind power generators and electric vehicles," IEEE Transactions on Smart Grid, vol. 4, no. 3, pp. 1314-1322, 2013.
9. R. A. Verzijlbergh, L. J. De Vries, and Z. Lukszo, "Renewable energy sources and responsive demand. Do we need congestion management in the distribution grid?," IEEE Transactions on Power Systems, vol. 29, no. 5, pp. 2119-2128, 2014.
10. J. Zhao, F. Wen, Z. Y. Dong, Y. Xue, and K. P. Wong, "Optimal dispatch of electric vehicles and wind power using enhanced particle swarm optimization," IEEE Transactions on Industrial Informatics, vol. 8, no. 4, pp. 889-899, 2012.
11. W. Shen and X. Cui, "Impact of electric vehicles and renewable energy systems on cost and emission of electricity," in 2012 7th IEEE Conference on Industrial Electronics and Applications (ICIEA), 2012, pp. 120-125: IEEE.
12. (2014). Power your Tesla with solar fuel. Available: ⟨http://solar.solarcity.com/promotions/tesla/⟩.
13. W. Su and M.-Y. Chow, "Performance evaluation of an EDA-based large-scale plug-in hybrid electric vehicle charging algorithm," Smart Grid, IEEE Transactions on, vol. 3, no. 1, pp. 308-315, 2012.
14. B. Deeks and L. White, "Particle Swarm Optimization," 2014.
15. M. Goonewardena and L. B. Le, "Charging of electric vehicles utilizing random wind: A stochastic optimization approach," in 2012 IEEE Globecom Workshops, 2012, pp. 1520-1525: IEEE.